Beni-Suef University Journal of Basic and Applied Sciences

RESEARCH

Open Access

Electrical properties of chelating copolymers and their metal complexes: binary chelating copolymers of styrene with organic acids

Mohamed Yahia[1,2*], Dalia Refaat[3,4], Gaber El-Enany[5,6] and Mahmoud Ahmed Abd El-Ghaffar[7*]

Abstract

Background The emulsion polymerization of vinyl monomers has been extensively researched, but copolymerization with crotonic acid or cinnamic acid is relatively uncommon. These acids are capable of coordinating with other metal ions. Our previous research has focused on synthesizing and characterizing copolymers of butyl acrylate (BuA)/vinyl acetate (VAc) and styrene-BuA using emulsion techniques, specifically for paint applications. The current work aimed to synthesize and characterize three binary chelating copolymers of styrene with maleic, cinnamic, and crotonic acids. In addition, the prepared chelating copolymers were treated with water and soluble salts of copper and iron for complex formation. Additionally, the characterization and electrical properties of these copolymers were investigated.

Results This article reports the synthesis of three binary copolymers of styrene with cinnamic, crotonic, and maleic acids via an emulsion polymerization process using a redox initiation system of potassium persulfate/glucose in the presence of sodium dodecyl benzene sulfonate as an emulsifier. The prepared emulsions of the copolymers were precipitated and purified using Soxhlet extraction in a mixture of n-hexane and toluene. Spectroscopic measurements, including Fourier transform infrared (FTIR), proton nuclear magnetic resonance (^{1}H-NMR), and powder X-ray diffraction (PXRD), in addition to thermal analysis methods like thermogravimetric analysis (TGA) and differential scanning calorimetry (DSC) were employed to characterize the copolymers that were synthesized. The metal complexes of the chelating copolymers were prepared by treatment with soluble metal salts of Co(II), Cu(II), and Fe(III), purified, and characterized via IR, PXRD, TGA, and DSC. The semiconducting properties of the chelating polymers and their metal complexes were demonstrated through conductivity measurements taken at room temperature. The conductivity values ranged from 10^{-3} to 10^{-6} Ω^{-1} cm^{-1}.

Conclusion The research underscores the significance of the electrical characteristics of chelating copolymers and their metal complexes, particularly focusing on styrene-based binary chelating copolymers, in driving advancements in technology, science, and economic development.

Keywords Chelating copolymer, Emulsion polymerization, Spectroscopic measurements, Semiconducting properties

*Correspondence:
Mohamed Yahia
mohamed.yahia@science.helwan.edu.eg; myahia@cicenergigune.com
Mahmoud Ahmed Abd El-Ghaffar
mghaffar50@yahoo.com
Full list of author information is available at the end of the article

1 Background

Functional and chelating polymers have shown great potential for various applications, including coatings on metal and glass surfaces, thermal lubricants and adhesives, semiconductors, and electrical insulators [1, 2]. Metal–polymer chelates have been used as electrochromic materials, as the polymer color changes with the metal ion's oxidation state in the chelate [3, 4]. Polymer–metal ligands are used to selectively remove trace contaminants from water [5–8]. Chelating resins containing active sites with different functionalities have been employed to bind a range of metal ions [9, 10]. The existence of carboxylic-COOH groups in the chelating polymer backbone allows for the formation of metal-acrylate by alkali-treatment [1, 5] or metal complexes by treating with certain transition-metal salts [1, 11, 12]. Furthermore, the physical properties of polymers, such as thermal stability, crystallinity, and strength, along with their chemical reactivity, are significantly altered by the inclusion of metal ions. This is one of the primary drivers behind the increasing benefit in polymer-metal complexes, particularly their catalytical capabilities in hydrogenation [1], oxidation [13–18], polymerization [1, 19, 20], paramagnetism [21], etc. Considering the potential applications in semiconductor materials and electronic plastic-materials, the characterization and investigation of the properties of chelating polymers are significant. Polymers that form complexes can be synthesized or produced from sustainable resources. In our study, we focused on the synthesizing a variety of innovative chelating resins containing different acrylic acid moieties copolymerized with the styrene monomer. After complexation with different transition-metal salts ($CuCl_2$ and $FeCl_3$), we investigated their electrical conductivity for their potential use as novel semiconductor materials. Numerous studies have been conducted on copolymers of styrene and maleic acid [22–24]. These copolymers are usually synthesized by the alkaline-hydrolysis of styrene maleic-anhydride copolymers and retain the alternating structure of their parent polymers. The emulsion polymerization of vinyl monomers has been extensively researched [25–27], but copolymerization with crotonic acid or cinnamic acid is relatively uncommon. These acids are capable of coordinating with other metal ions [28–30]. Our previous research has focused on synthesizing and characterizing copolymers of Butyl Acrylate (BuA)/Vinyl Acetate (VAc) and Styrene-BuA using emulsion techniques, specifically for paint applications [31, 32].

The current work aimed to synthesize and characterize three binary chelating copolymers of styrene with maleic, cinnamic, and crotonic acids. In addition, the prepared chelating copolymers were treated with water and soluble salts of copper and iron for complex formation. Furthermore, the characterization and electrical properties of these copolymers were investigated.

2 Methods

2.1 Materials

Merck-Schuchardt in Germany provided styrene (St), cinnamic acid (CA), maleic acid (MA), crotonic acid (CrA), and potassium persulfate (KSP). Before use, the styrene monomer was redistilled and stored at − 20 °C. Sodium dodecyl benzene sulfonate (SDBS) and glucose were obtained from the Egyptian El-Nasr chemical company. Distillation was used to purify water for all experiments.

2.2 Preparation methods

A semi-batch emulsion copolymerization process was conducted to produce binary copolymers of styrene with maleic acid (MA), cinnamic acid (CA), and crotonic acid (CrA). The ingredients, including an initiation redox system of KPS/Glucose (0.270 g/0.018 g), 1.0 g of sodium dodecylbenzenesulfonate (SDBS) as an emulsifier, and 86–89 mL of distilled water, were mixed in a three-necked flask (500 mL). Equimolar ratios of MA, CA, and CrA (5.0 mmol) with styrene (5.0 mmol) were synthesized by gradually dropping the acidic monomer to the hydrophobic polymerized styrene monomer in the reaction mixture after 30 min. The polymerization reactions were performed with mechanical agitating at (500 rpm and 65 °C) for 4 h.

2.3 Instrumental analysis

Perkin-Elmer FTIR was utilized to conduct an IR analysis of the prepared polymers at the Micro-Analytical Unit (Nagano, Japan) located in the Faculty of Science at Cairo University. In addition, a thermogravimetric analysis (TGA) was conducted on the polymers by utilizing a thermal analysis system (Perkin-Elmer 7 series/Shimadzu-TGA 50 H) with a constant rate of nitrogen. Furthermore, Scanning Differential Calorimetry-DSC was conducted at a constant nitrogen rate using Perkin-Elmer 7 series/Shimadzu-DSC 50 H thermal analysis systems from (Nagano, Japan). The prepared polymers were also analyzed using ^{1}H-NMR spectra (a JEOL EX-270 NMR) spectrophotometer at 270 MHz, which included a superconducting magnet (Oxford) and a 5-mm dual probe for ^{1}H-NMR analysis. The standard conditions for the ^{1}H-NMR analysis included a spectral width of 4000 Hz for ^{1}H and a flip angle (45°).

2.4 Measurements of electrical conductivity

Hioki 3532–50 Hitester version 131 from Hioki E.E. Corporation, Nagano, Japan, was used to measure electrical

properties. This device can measure frequencies between 42 Hz and 5 MHz and signal levels ranging from 1 mV to 5 V, with a maximum current of 99 mA. Prior to conducting measurements, the powdered samples were compressed with a force of 10 tons/cm^2 to produce pellets with a 13 mm diameter and a 1–3 mm thickness. Both sides of the pellets were coated with silver paint and tested for conductivity. The study measured four electrical parameters impedance Z, parallel equivalent static capacitance Cp, phase angle, and parallel equivalent bulk resistance (Rp) of the samples in 42 Hz to 6 MHz frequency range.

Measurements of conductivity at different temperatures were performed. The cell used consists of a simple holder and furnace. The furnace used for heating was designed so that no e.m.f is induced in the measured sample. The measurements were conducted upon a range of temperature (30–100 °C) using a temperature control unit with a stability of ± 0.5 °C. The sample was subjected to heating at a slow heating rate and allowed to stand at the desired temperature for 1 min before measurement to achieve a constant interruption of heat in the sample.

3 Results

3.1 Synthesis of styrene copolymers

Three copolymers, namely, St-co-MA, St-co-CA, and St-co-CrA, were synthesized using an initiation redox system (KPS/Glucose) at a temperature of 65 °C. The (%) conversion as a time function is shown in Fig. 1**.**

The designed copolymer structures of St-co-MA, St-co-CA, and St-co-CrA are presented in Fig. 1**.** The structures of previous chelating copolymers with various metal ions (copolymer–metal complexes) formed by inter-molecular and/or intra-molecular bridging ligands are shown in Scheme 1 [5].

3.2 The synthesized copolymers' characterization and their metal complexes

3.2.1 H-NMR spectroscopy

The composition and chemical configurations of the produced copolymers were determined by ^{1}H-NMR spectroscopy based on the recorded characteristic bands illustrated in Table 1. The spectra of the three binary chelating copolymers are presented in Fig. S1 *(See the supplement information-SI).*

3.2.2 FTIR-spectroscopy

The FTIR spectra analysis for St-co-MA, St-co-CA, and St-co-CrA copolymers is illustrated in Table 2**.** The spectra of the three copolymers are presented in Figs. S2-S4 *(See the supplement information-SI).*

3.2.3 XRD—powder diffraction analysis

The dA^o values and relative intensities (I/I$_o$) of the XRD patterns of the St-co-MA, St-co-CA, and St-co-CrA copolymers and their copper and iron metal complexes are represented in Table 3 and are presented in Figs. S5–S7 *(See the supplement information-SI).*

3.2.4 TGA—thermal gravimetric analysis

The TGA diagrams of the St-co-MA and St-co-CrA copolymers are illustrated in Fig. 2a, b, respectively.

3.2.5 Scanning differential calorimetry (DSC)

The glass transition temperatures (Tg) of the copolymers and their metal complexes were assessed by subjecting them to heating from room temperature (r.t) to 500 °C with a heating rate of 10 °C/min in dry N_2 gas using crimped aluminum pans as represented in Table 4**.**

3.3 Electrical conductivity properties

3.3.1 DC electrical conductivity

The electrical conductivity of both the copolymers and their corresponding metal complexes containing Cu(II) and Fe(III) was investigated. The DC electrical conductivity was evaluated over a range of temperature from 30 to 100 °C, and its temperature dependence is described by the following expression:

$$\boldsymbol{\sigma}_{\boldsymbol{T}} = \boldsymbol{\sigma}_{\circ} \exp\left(-\boldsymbol{E_a}/\boldsymbol{KT}\right) \tag{1}$$

where (E_a): The electrical conduction thermal energy, (K): the constant of Boltzmann, (T): temperature (Kelvin), and ($\boldsymbol{\sigma}_{\circ}$): The semiconductor nature parameter. The values of E_a are based on the polymer molecular configuration. The conductivity of the polymers and their metal complexes were in the range of semiconductor materials (10^{-6}–10^{-7} Ω^{-1} cm^{-1}), as reported in Table 5**.**

3.3.2 AC electrical conductivity

The AC electrical conductivity characteristics of the produced samples are displayed in Fig. 7**.** The outcomes obtained can be explained in the following manner. The conductivity of σ(ω), which is dependent on the frequency, can be shown as the combination of two factors [35]:

$$\sigma(\omega) = \sigma_o + \sigma_{AC}(\omega) \tag{2}$$

where the DC conductivity (σo) is frequency-independent, and the AC conductivity ($\sigma_{AC}(\omega)$) increases with frequency.

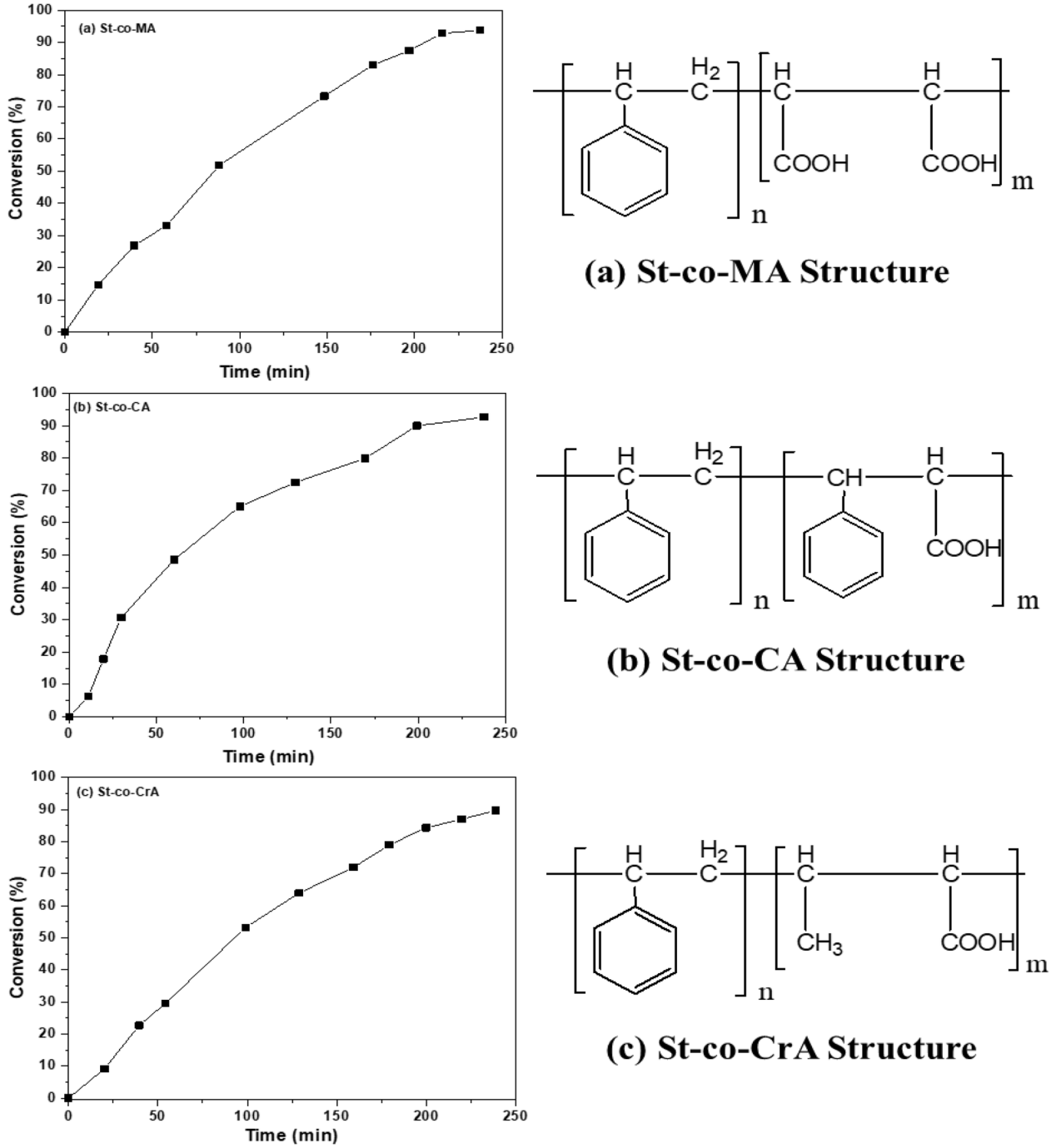

Fig. 1 The emulsion copolymerization conversion curves for **a** St-co-MA, **b** St-co-CA, and **c** St-co-CrA at 65 °C

4 Discussion

4.1 The copolymer and the metal complexes' characterizations

As shown in Scheme 1, the proposed mechanism of polymerization between styrene and maleic acid (MA), cinnamic acid (CA), and crotonic acid (CrA) as well as the subsequent coordination of Fe(III) and Cu(II) metal ions with the polymer. The polymerization follows a free-radical mechanism, initiated by a radical species that attacks the vinyl groups of styrene, CA, and CrA, resulting in alternating copolymerization. The figure highlights how the presence of electron-withdrawing groups in MA

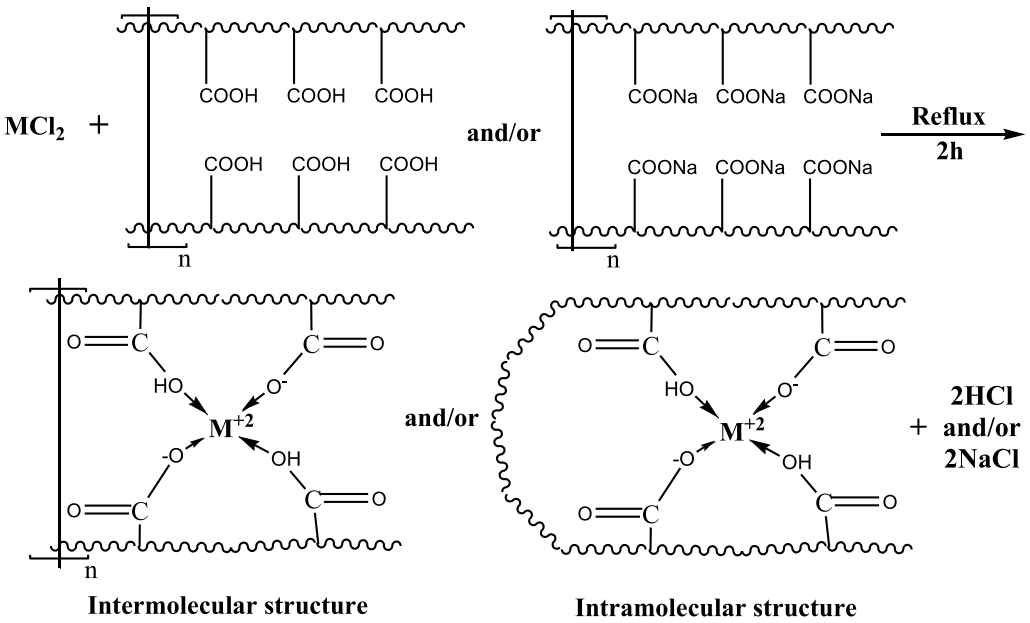

Scheme 1 Reaction of chelating copolymers with metal salts

and CA stabilizes the growing polymer chain, while the coordination of metal ions occurs at the carboxylate sites (-COOH) of MA and CA. This metal complex formation contributes to the enhanced crystallinity and thermal stability of the material, as observed in the thermal analysis (TGA and DSC). The coordination between metal ions and the carboxylate groups leads to cross-linking, thus reinforcing the polymer structure, which is further validated by the 1H-NMR and FTIR spectra, showing shifts in COO − stretching frequencies.

As shown in Fig. 1 (the percentage of polymer conversion as a time function), It is clearly realized from the conversion time curves that the plateau representing the initial rate of polymerization of St-co-MA, St-co-CA, and St-co-CrA increases sharply with time until it reaches a maximum value greater than 90% conversion within 2–4 h. Subsequently, the plateau reaches a steady state, and the reaction yield falls between the range of 85–92%.

^{1}H-NMR spectra (Fig. S1 and Table 1) for the three copolymers (St-co-MA, St-co-CA, and St-co-CrA) showed expected signals for the phenyl groups at (6.55–7.065 ppm) and the aliphatic (-CH-) groups at (2.0–2.4 ppm). For (St-co-CrA), there is a new peak at (1.2–1.5 ppm) for the methyl (-CH_3) groups. For the (St-co-CA) copolymer, there is a new peak appears at (7.4–7.68 ppm) for the benzene ring within the copolymer architecture. Table 1 and Fig. S1 provide clear evidence for successful incorporation of the crotonic and cinnamic acids into the copolymer matrix, further reinforcing the polymer's structure as hypothesized.

Additionally, the functional groups in the structures of the three copolymers and their metal complexes exhibit comparable characteristic peaks in the FTIR spectra (Fig. S2). These peaks include expected signals for the (OH-carboxylic group) and (M–O groups) at (3400–3500 cm^{-1}) and (450–550 cm^{-1}), respectively. Notably, the existence of (OH-carboxylate) in the copolymers is evident, whereas it is absent in the metal complexes. In the opposite way, (M–O groups) are absent in the copolymers but present in the metal complexes. Table 2 and Fig. S2 support convincing evidence for the formation of all three copolymers and their complexes. It is clearly seen from Figs. S2-S4 that the bands at 1717–1690 cm^{-1} reveal the existence of carbonyl groups of carboxylic acids, and other characteristic bands at 2925–2825 cm^{-1} demonstrate the existence of CH, CH_2, and CH_3 groups. The bands at 3060 cm^{-1} imply the existence of CH stretching of the phenyl groups, and the extensive band around 3440 cm^{-1} demonstrates the existence of the OH group of the carboxylic function of maleic, cinnamic, and crotonic acids. The FTIR-spectroscopy was enhanced for the characterization of the prepared copolymers, as illustrated in Table 2**.** The IR spectra of the prepared copper and iron metal complexes of St-co-MA, St-co-CA, and St-co-CrA copolymers are presented in Table 2 and Figs. S3 and S4 *(the supplement information-SI).*

Table 1 The chemical shifts of the binary chelating copolymers

Resonance signal (ppm)	Proton	Assignment
Chemical shifts of St-co-MA copolymers		
6.55–7.065	Styrene (5H) (2d, 2t, t)	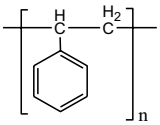
2.0–2.4	– (CH) – (α) (1H St + 1H MA) d, d	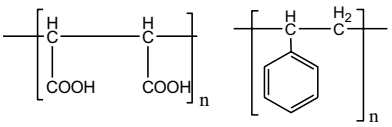
Chemical shifts of St-co-CA copolymers		
7.4–7.68	Cinnamic acid (5H)	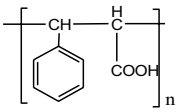
6.55–7.065	Styrene (5H) (2d, 2t, t)	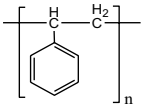
2.0–2.4	– (CH) – (α) (1H St + 1H CA) d, d	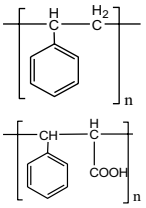
Chemical shifts of St-co-CrA copolymers		
6.55–7.065	Styrene (5H) (2d, 2t, t)	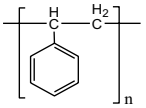
2.0–2.4	– (CH) – (α) (1H St + 1H CrA) d, d	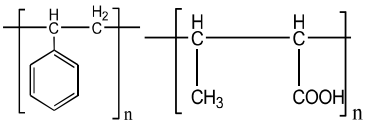
1.2–1.5	CH3 (3H CrA) d	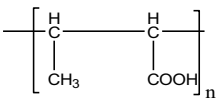

These spectra provide valuable details regarding the prepared polymer–metal complexes' backbones. The bands at 1684–1633 cm^{-1} demonstrate the existence of a carboxylate anion (COO^{-}), which slightly shifted due to the complexation of the copolymers with Fe(III) and CU (II) ions through the carboxyl groups. An extra band at 540–418 cm^{-1} implies the presence of a metal–oxygen bond. Table 2 also lists the recognized bands of the synthesized polymer complexes of Fe(III) and Cu(II) ions, as shown in Figs. S3 and S4 (see *the supplement information-SI*). Table 2 presents good evidence for the formation of the three binary chelating copolymers and their metal complexes.

Additionally, Table 3 and Figs. S5-S7, there is a slight variation in the values of dA° and the appearance of new peaks for St-co-MA, St-co-CA, and St-co-CrA copolymers and their copper and iron metal complexes, as shown in the figures, which were attributed to the variety

Table 2 FTIR spectra of three copolymers and their metal complexes

	OH-carboxylic group	CH – Aromatic stretching	CH – aliphatic stretching	CH_2 – aliphatic stretching	C = O carbonyl group	C = C aromatic stretching	M–O chelating bond
St-co-MA	3446	3059	2920	2850	1690	1598	–
St-co-CA	3442	3060	2924	2852	1692	1627	–
St-co-CrA	3436	3059	2921	2851	1717	1599	–
St-co-MA/Cu	–	3059	2920	2850	1655	1598	539
St-co-CA/Cu	–	3060	2924	2852	1633	1627	539
St-co-CrA/Cu	–	3059	2921	2851	1677	1599	540
St-co-MA/Fe	–	3059	2920	2850	1662	1598	418
St-co-CA/ Fe	–	3060	2924	2852	1641	1627	482
St-co-CrA/ Fe	–	3059	2921	2851	1684	1599	538

Table 3 X-ray diffraction data for St-co-MA, St-co-CA, St-co-CrA, and their complexes

St-co-MA						St-co-CA						St-co-CrA					
Pure		Cu(II) Complex		Fe(III) Complex		Pure		Cu(II) Complex		Fe(III) Complex		Pure		Cu(II) Complex		Fe(III) Complex	
dA°	I/I_o	dA°	I/I_o	dA°	I/I_o	dA°	I/I_o	dA°	I/I_o	dA°	I/I_o	dA°	I/I_o	dA°	I/I_o	dA°	I/I_o
–	–	–	–	–	–	19.412	–	19.41	6.4	19.41	–	–	–	–	–	–	–
–	–	–	–	–	–	16.007	–	16.00	–	16.007	84.5	–	–	–	–	–	–
–	–	–	–	–	–	15.561	–	15.56	14.4	15.56	–	–	–	–	–	–	–
–	–	–	–	–	–	13.953	–	13.95	62	13.95	–	–	–	–	–	–	–
–	–	–	–	–	–	11.249	–	11.25	–	11.24	100	–	–	–	–	–	–
–	–	–	–	–	–	8.983	80	8.983	79.3	8.983	–	–	–	–	–	–	–
7.137	–	7.137	59.9	7.137	–	8.381	–	8.381	20.2	8.381	48.2	–	–	–	–	–	–
–	–	–	–	–	–	6.200	–	6.200	–	6.200	61.7	–	–	–	–	–	–
–	–	–	–	–	–	5.855	22.1	5.855	30.8	5.855	82	5.465	–	5.465	100	5.465	–
4.243	–	4.243	100	4.243	–	4.810	65.3	4.810	94.1	4.810	61.7	–	–	–	–	–	–
–	–	–	–	–	–	4.732	44.9	4.732	83.6	4.732	–	–	–	–	–	–	–
–	–	–	–	–	–	4.494	33.5	4.494	61.3	4.494	–	–	–	–	–	–	–
–	–	–	–	–	–	4.303	34.1	4.303	57.5	4.303	–	–	–	–	–	–	–
–	–	–	–	–	–	4.103	37.5	4.103	61	4.103	–	–	–	–	–	–	–
–	–	–	–	–	–	3.885	100	3.885	100	3.885	–	3.458	–	3.458	57.6	3.458	–
–	–	–	–	–	–	3.512	79.2	3.512	95.1	3.512	–	–	–	–	–	–	–
3.377	–	3.377	93.9	3.377	–	3.279	17	3.279	32.9	3.279	82.9	–	–	–	–	–	–
–	–	–	–	–	–	3.028	48.7	3.028	54.4	3.028	–	–	–	–	–	–	–
–	–	–	–	–	–	2.791	12.7	2.791	–	2.791	44.6	2.820	–	2.820	50.7	2.820	–
2.691	–	2.691	35.6	2.691	–	2.644	10.5	2.644	24.9	2.644	56.3	2.771	–	2.771	42.8	2.771	–
2.174	–	2.174	33	2.174	–	2.244	8.4	2.244	–	2.244	45.9	2.267	–	2.267	34.4	2.267	–
–	–	–	–	–	–	1.850	–	1.850	16.8	1.850	24.8	–	–	–	–	–	–
–	–	–	–	–	–	1.643	–	1.643	–	1.643	36	–	–	–	–	–	–

of metal ions existing in the copolymers. The figures illustrate a low degree of crystallinity for the prepared copolymers and a moderate degree of crystallinity for their metal complexes. It is also shown that the degree of crystallinity of the styrene/cinnamic acid copolymer and its copper and iron metal complexes is higher than that of the styrene/maleic acid and styrene/crotonic acid copolymers and their copper and iron metal complexes, and this is attributed to the crystallinity of the styrene crotonic copolymer. Additionally, the copolymers are typically amorphous, and their complexation with metal ions (iron and copper) potentially improves their crystallinity;

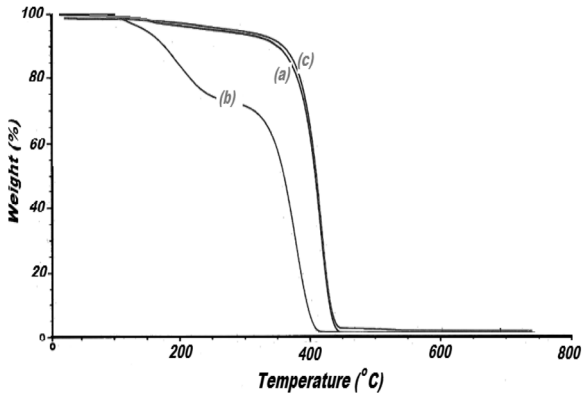

Fig. 2 TGA diagram for binary copolymers of **a** St-co-MA, **b** St-co-CA, and **c** St-co-CrA

Table 4 DSC data for styrene/maleic acid, styrene/cinnamic acid, and styrene/crotonic acid copolymers and their complexes

Copolymer	(Tg) Value (°C)		
	Pure	Cu(II) Complex	Fe(III) Complex
St-co-MA	103.92	125.49	105.31
St-co-CA	105.72	131.40	161.73
St-co-CrA	98.38	105.00	96.89

Table 5 Electrical conductivity and calculated activation energies for the prepared polymer samples

Sample	$\sigma_{40}(\Omega^{-1}.cm^{-1})$	Range, T (°C)	Ea (eV)
St-co-CA	2×10^{-6}	30–100	0.140
St-co-CA/Na	5×10^{-7}	30–100	0.136
St-co-CA/Cu(II)	2×10^{-7}	30–50	0.590
		50–100	0.009
St-co-CA/Fe(III)	5×10^{-7}	30–80	1.100
St-co-CrA	4×10^{-6}	30–60	1.20
		60–100	0.28
St-co-CrA/Na	5×10^{-7}	30–100	0.26
St-co-CrA/Cu(II)	3.2×10^{-7}	30–60	0.38
		60–100	0.00
St-co-CrA/Fe(III)	4×10^{-7}	30–80	0.19

as shown in the figures, there is a significant increase in crystallinity upon complexation with metal ions. While there may be some slight improvement in crystallinity compared to the amorphous copolymer, the degree of crystallinity was still relatively low, as previously noted.

The spectral properties of the copolymers and their metal complexes, as shown through FTIR, NMR, and X-ray diffraction analyses, offer valuable insights into their structural organization. From the 1H-NMR data, distinct chemical shifts, such as those for phenyl and aliphatic groups, confirm the presence of styrene units, while additional signals verify the successful incorporation of crotonic and cinnamic acids into the copolymer matrix. The FTIR spectra further validate this, with key bands indicating hydroxyl, carboxyl, and carbonyl groups in the un-complexed copolymers. Upon metal complexation with Fe(III) and Cu(II), shifts in these bands, particularly the appearance of metal–oxygen stretching, indicate the coordination of metal ions with carboxylate groups, forming stable metal–oxygen bonds. X-ray diffraction data reveal that the copolymers are largely amorphous, but complexation with metal ions increases crystallinity, especially in styrene-cinnamic acid copolymers. This improvement in crystallinity is attributed to the role of metal ions as cross-linking agents, promoting a more organized polymer matrix. In conclusion, the combination of NMR, FTIR, and X-ray data demonstrates how the structural features of the copolymers influence their coordination with metal ions. These structural transformations enhance thermal stability and crystallinity, emphasizing the crucial link between structure and function in determining the material properties.

Figure 2a, b illustrates the thermal stability for (St-co-MA and St-co-CrA), as shown in Fig. 2, the two copolymers retain their initial masses from room temperature up to 380 °C (there is only a slight amount of water loss, around 4.0% weight loss), which may be due to water contamination with the polymer (creation of H-bonds between the polymer matrix and the water molecules), after which the two copolymers show a complete sharp decomposition in their masses. On the other hand, the TGA diagram for the styrene/cinnamic acid copolymer (Fig. 2b) shows that it retains its initial mass up to 100 °C, after which the polymer shows gradual degradation from 100 °C up to 320 °C, where it loses about 30% of its initial mass. This may be due to decarboxylation, which is more easily decomposed through carbanion formation stabilized by the – I effect of the phenyl group. After that, the polymer began to undergo a sharp decomposition from 320 to 425 °C.

Furthermore, the TGA curve of the St-co-MA/Cu(II) complex is demonstrated in Fig. 3a. The Cu(II) complex shows a slight loss of about 4% of its initial mass from room temperature up to 170 °C due to water (H_2O) molecules bound with the polymer–metal complex structure. After that, the polymer shows a gradual decomposition from 170 °C up to 380 °C, where it loses about 25% of its initial mass. From 320 °C to 425 °C, a sharp decomposition occurs for the polymer complex, where the complex retains about 15% of its initial mass due to metal oxide formation. This complex shows higher weight loss compared to the St-co-CrA/Cu(II) complex due to a higher

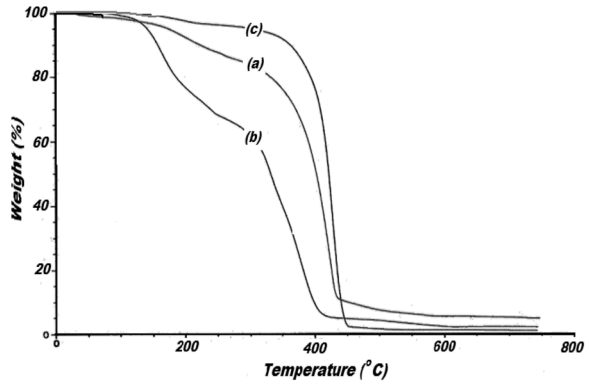

Fig. 3 TGA diagram for copolymer copper complex of **a** St-co-MA/Cu(II), **b** St-co-CA/Cu(II), and **c** St-co-CrA/Cu(II)

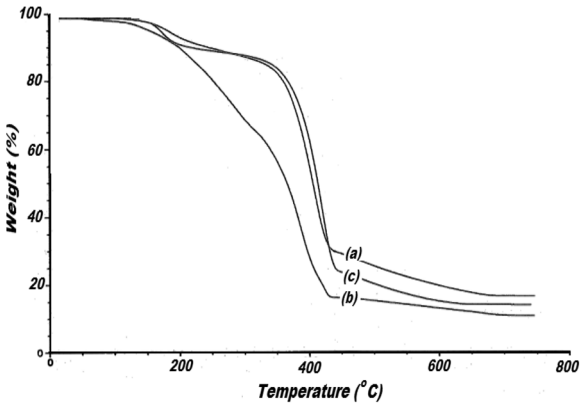

Fig. 4 TGA diagram for copolymer iron complex of **a** St-co-MA/Fe(III), **b** St-co-CA/Fe(III), and **c** St-co-CrA/Fe(III)

amount of bound water, as evidenced by the IR spectra illustrated in Fig. 3. Additionally, the TGA diagram of the St-co-CA/Cu(II) complex is demonstrated in Fig. 2b; as shown in the diagram, it undergoes a slight loss of about 3% of its initial mass from room temperature up to 150 °C. After that, the polymer shows a gradual decomposition from 150 °C up to 325 °C, where it loses about 40% of its initial mass due to decarboxylation. From 325 to 430 °C, a sharp decomposition occurs for the polymer complex. The diagram shows that the complex retains about 10% of the initial mass due to metal oxide creation. Also, the TGA curve of the St-co-CrA/Cu(II) complex is explained in Fig. 3c. It is obvious in the figure that the copolymer complex maintains its initial weight up to 100 °C. After that, the copolymer complex shows a slight loss of about 10% of its initial mass from room temperature up to 380 °C. Figure 3 illustrates that the thermal performance of the St-co-CrA/Cu(II) copper metal complex is quite similar to the thermal performance of the St-co-MA/Cu(II) complex. Additionally, the figure demonstrates that the St-co-CA/Cu(II) complex has lower thermal stability than the St-co-MA/Cu(II) and St-co-CrA/Cu(II) complexes.

Furthermore, the TGA curve of the St-co-MA/Fe(III) complex is demonstrated in Fig. 4a. The copolymer complex shows a slight loss of about 5% of its initial mass from room temperature up to 180 °C, after which the complex shows a gradual decomposition from 180 °C up to 340 °C, where it loses about 20% of its initial mass. From 340 to 425 °C, a sharp decomposition occurs for the copolymer complex. The diagram also shows that the complex retains about 30% of the initial mass of the copolymer complex due to metal oxide decomposition. The TGA curve of the St-co-CrA/Fe(III) complex is explained in Fig. 4c; the copolymer complex shows a slight loss of about 5% of its initial mass at room temperature up to 175 °C. Then, the copolymer complex shows a gradual decomposition from 175 °C up to 350 °C, where it loses about 17% of its initial mass. From 350 to 450 °C, a sharp decomposition occurs for the copolymer complex. The curve also shows a slight decomposition at 25% of the initial mass of the copolymer complex due to the decomposition of the metal oxide. Also, the TGA curve of the St-co-CA/Fe(III) complex is explained in Fig. 4b; the copolymer complex shows a slight loss of about 3% of its initial mass from room temperature up to 140 °C. Then, the polymer shows a gradual decomposition from 140 °C up to 440 °C, where it loses about 85% of its initial mass. The curve also shows a slight decomposition of 15% of the initial mass of the copolymer complex due to metal oxide decomposition. Figure 4 illustrates that the thermal behavior of the St-co-CrA/Fe(III) complex is quite similar to the thermal behavior of the St-co-MA/Fe(III) complex. The figure also illustrates that the thermal stability of the St-co-CA/Fe(III) complex is lower than that of the St-co-MA/Fe(III) and St-co-CA/Fe(III) complexes. Additionally, the TGA curves for the three copolymers and their metal complexes indicate weight losses between 100 and 200 °C for both the copolymers and their metal complexes, which can be ascribed to the elimination of bound water and other volatile contaminants within the copolymers' backbones.

Furthermore, Table 4 represents the DSC results, the obtained results indicated that the St-co-CA copolymer and its copper and iron metal complexes display higher Tg than the St-co-MA and St-co-CrA copolymers and their copper and iron metal complexes. The recorded DSC thermal analysis data are aligned with the TGA findings as shown in Figs. 2–4.

The thermal analysis of the copolymers (St-co-MA, St-co-CA, St-co-CrA) and their metal complexes through TGA and DSC provides significant insights into their

structural stability. The copolymers exhibit stability up to 380 °C, with minor water loss attributed to hydrogen bonding, followed by sharp decomposition. Among the copolymers, St-co-CA shows earlier degradation, likely due to decarboxylation effects. Metal complexation, particularly with Fe(III) and Cu(II), improves thermal stability by forming stable metal–oxygen bonds, increasing decomposition temperatures to 425–450 °C due to cross-linking. The enhanced crystallinity and higher glass transition temperatures, particularly in the St-co-CA complexes, are linked to the rigidity and structural order induced by the cinnamic acid moieties. This study highlights the critical role of metal coordination in boosting thermal properties, making these materials promising candidates for applications requiring high thermal resistance.

4.2 The electrical conductivity characterization

Polymer complexes are known to contain adsorbed water (H_2O) molecules owing to these compounds having high polarity, as previously noted by Patel and Patil [33], who stated that this property may have a possible effect on the bulk DC electric conductivity. As shown in the FTIR spectra of copolymer complexes (Figs. S3 and S4**,** *see the supplement information-SI*), the characteristic band of contaminated water can be noted in the region of 3000–3400 cm^{-1} as mentioned in Sect. (3.2.2).

Figure 5 appears the curves of log $\boldsymbol{\sigma}$ vs. (1/T (K)) for the St-co-CA, St-co-CA sodium salt, and St-co-CA complexes with Cu(II) and Fe(III). One can see that the DC conductivity of St-co-CA and its sodium salt is higher than the DC conductivity of the corresponding complexes. Additionally, the activation energies of St-co-CA and its sodium salt are lower than the activation energies of the corresponding complexes, which may be due to the higher ionic mobility of H^+ and Na^+, which increase the ionic conductivity. In addition, the samples show semiconducting performance, whereby their conductivity rises with a rise in temperature. However, in the case of Fe (III)/copolymer complexes, as shown in Figs. 5 and 6, we can observe that the log $\boldsymbol{\sigma}$ vs. (1/T (K)) curves have two segments in the temperature ranges 30–80 °C and 80–100 °C. The first segment displays a negative slope, indicating that the DC conductivity increases with increasing temperature, while the second segment has a positive slope, indicating a decrease in DC conductivity within this range. This unexpected behavior can be explained by El-Shekel et al.'s model [34], which proposes that the temperature dependence of electrical conductivity can be expressed as $\boldsymbol{\sigma_T = \sigma_\circ \exp\{-(E_1 - E_2)|KT\}}$.

In this temperature range, the energy of activation in the dry-state (E_1) and the energy associated with the process of re-combination between an electron and its corresponding hole released from a neutral polaron (E_2) play significant roles in the behavior of the log σ vs. (1/T) curves. E_2, which is associated with the polarons numbers emitted by water elimination or relaxation of chain, is greater than E_1, leading to a positive slope in the log σ vs. (1/T) curve when re-combination is the principal process. As the temperature increases, there is a decrease in the charge carriers' numbers, resulting in this behavior. The situation involves two polarons, one associated with adsorbed water and the other associated with chain conformation.

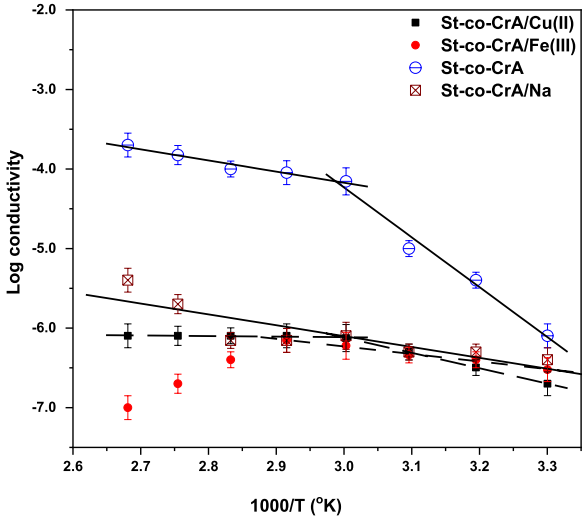

Fig. 5 Log $\boldsymbol{\sigma}$ vs. (1/T) curves for St-co-CA, St-co-CA/Na, and St-co-CA complexes with Cu(II) and Fe(III)

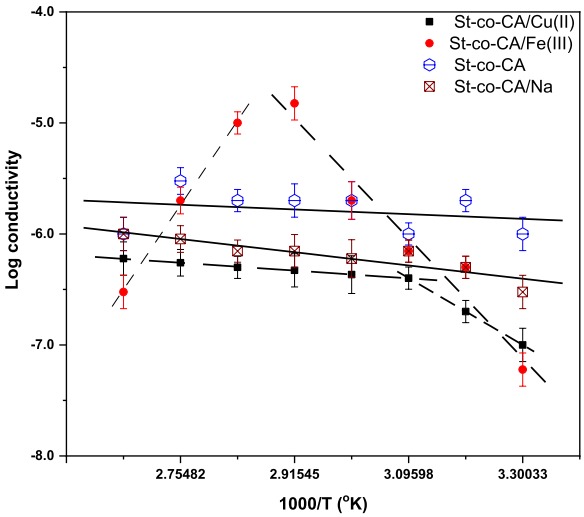

Fig. 6 Log $\boldsymbol{\sigma}$ vs. (1/T) curves for St-co-CrA, St-co-CrA/Na, and St-co-CrA complexes with Cu(II) and Fe(III)

In the case of the Cu(II)/St-co-CA complex (Fig. 5), one can note that the log $\boldsymbol{\sigma}$ vs. *(1/T (K))* curve possess two segments in the temperature ranges 30–50 °C and 50–100 °C with activation energies of 0.590 and 0.009 eV, respectively. Additionally, for the Cu (II)/St-co-CrA complex (Fig. 6), the log $\boldsymbol{\sigma}$ vs. (1/T (K)) curve has two segments: the first one is in the temperature range 30–60 °C, which exhibits an activation energy (Ea) = 0.38 eV, while the second range 60–100 °C is temperature-independent. In Fig. 6, St-co-CrA shows two distinct segments in the *log σ vs. (1/T (K))* graph. The first segment occurs between 30 and 60 °C, while the second occurs between 60 and 100°C. The points at which log σ vs. (1/T (K)) exhibits a change in slope may associated with the temperature at which the main chain CH_3-groups on the St-co-CrA molecule start to rotate. We suggest that the rotation of the main chain CH_3-groups results in the "cooperative movement of the main chain", which could cause the reorientation of polymer chains in relation to each other. This reorientation may modify the tunneling junctions by altering the distance between copolymer chains.

Additionally, Fig. 7 displays the frequency-dependent behavior of σAC(ω) at various temperatures. The data in Fig. 7a–f, h coincide, indicating that σAC(ω) is independent of temperature. Conduction at low temperatures can be attributed to electron hopping under the action of the electric field. Thermal activation is more effective at higher temperatures, and the conduction in this region can be attributed to polarization conduction, in addition to electron-hopping conduction. The AC conductivity rises with the increase in the frequency based on the equation [36]:

$$\sigma_{AC} = A\omega^{n} \tag{3}$$

The equation includes two parameters: A, which depends on temperature, and n, which is independent of temperature and has a value between 0 and 1. The frequency exponent, n, was determined by calculating the slopes of the straight lines, and the average value was found to be 0.99. In the case of the St-co-CrA copolymer in Fig. 7g, the value of n diminishes with rising temperature, from unity at room temperature (r.t.) to 0.60 at 100 °C.

Furthermore, the emulsion polymerization of styrene with maleic, cinnamic, and crotonic acids for metal complexation has not been extensively explored, particularly in comparison with more common monomers like butyl acrylate and vinyl acetate. Previous studies on copolymers of styrene and maleic acid have demonstrated moderate thermal stability and low crystallinity [37–40], similar to our findings, but their electrical properties were not extensively analyzed. In contrast, our work highlights the semiconducting nature of these copolymers, which aligns with studies on chelating polymers used in electronic applications [37–40]. Furthermore, the electrical conductivity values obtained for the metal complexes (ranging from 10^{-3} to 10^{-6} Ω^{-1} cm^{-1}) are comparable to those reported in the literature for polymer-metal complexes, such as polypyrrole and polyaniline complexes, which also exhibit semiconducting behavior under similar conditions [37–40]. The enhancement in thermal stability through metal complexation, particularly with copper and iron, has been corroborated by previous studies, which report similar shifts in degradation temperatures and crystallinity improvements upon metal coordination. By incorporating these comparisons, our study builds on and extends the understanding of polymer-metal complex systems, showcasing the unique properties of styrene-based chelating copolymers. This discussion strengthens the context of our findings and highlights the novelty and significance of the copolymers synthesized in this work.

5 Conclusion

This study involved the synthesis of three binary chelating copolymers using styrene with maleic acid, cinnamic acid, and crotonic acid through semi-batch emulsion copolymerization, followed by complex formation with water-soluble cobalt, copper, and iron salts. The resulting polymer–metal complexes were analyzed for their thermal stability and characterized using spectrometric techniques such as ^{1}H-NMR, FTIR, and PXRD. The structural features of the copolymers were confirmed by ^{1}H-NMR, where distinct chemical shifts corresponding to phenyl, aliphatic, and additional functional groups evidenced the successful incorporation of comonomers like crotonic and cinnamic acids. FTIR spectra further validated the presence of hydroxyl, carboxyl, and carbonyl groups in the copolymers and demonstrated significant shifts upon metal complexation, indicating coordination of the carboxylate groups with Fe(III) and Cu(II) ions. X-ray diffraction revealed an increase in crystallinity upon complexation, particularly for the styrene-cinnamic acid copolymers, due to metal-induced cross-linking. These results highlight the relationship between structural features and the enhanced stability and ordering observed in the polymer-metal complexes.

Furthermore, the thermal analysis of the copolymers (St-co-MA, St-co-CA, St-co-CrA) and their metal complexes through TGA and DSC provides significant insights into their structural stability. The copolymers exhibit stability up to 380 °C, with minor water loss attributed to hydrogen bonding, followed by sharp decomposition. Among the copolymers, St-co-CA shows

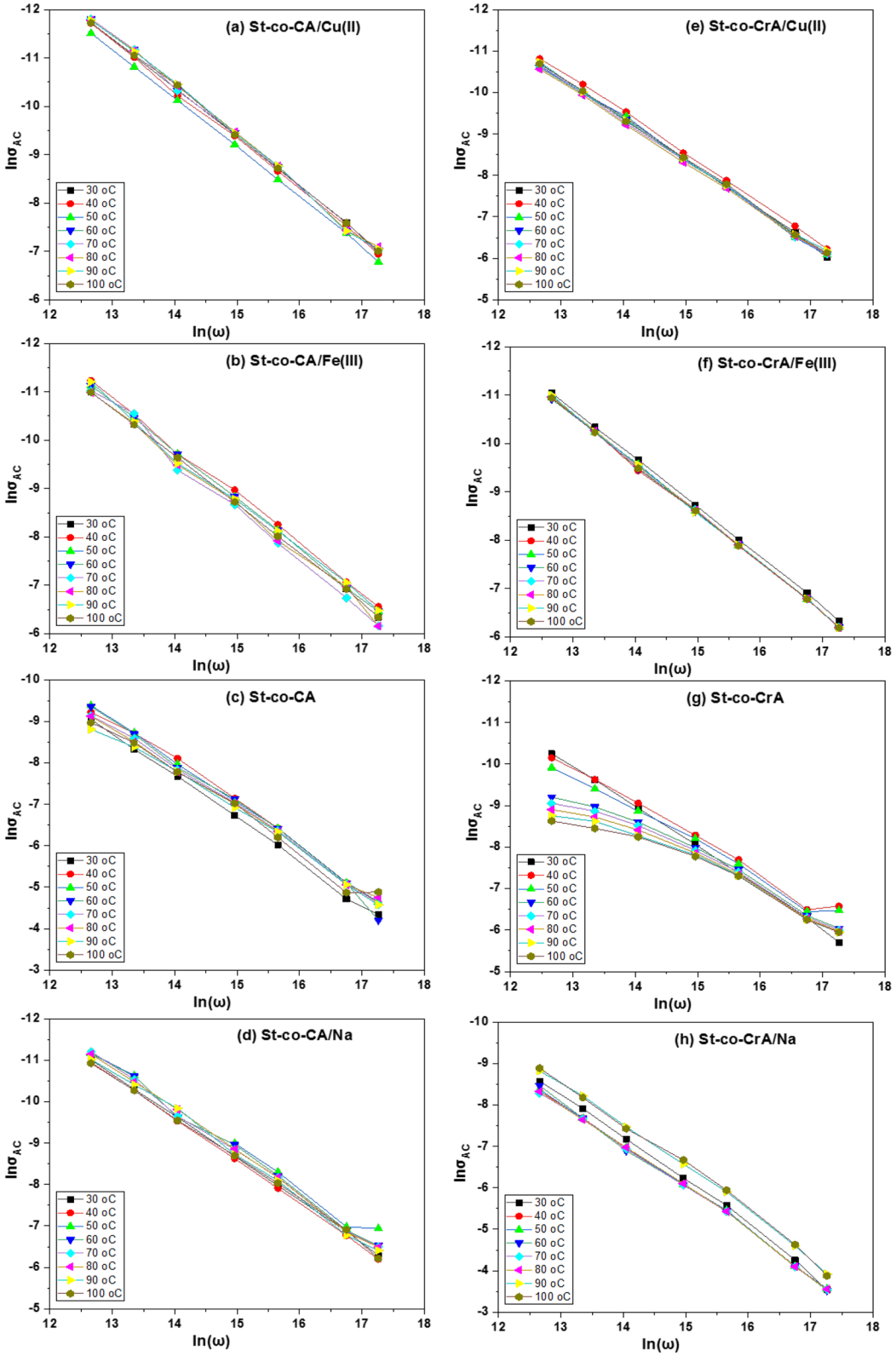

Fig. 7 The AC conductivity's frequency dependence at different temperatures (30–100 °C) for **a** St-co-CA/Cu(II), **b** St-co-CA/Fe(III), **c** St-co-CA, **d** St-co-CA/Na, **e** St-co-CrA/Cu(II), **f** St-co-CrA/Fe(III), **g** St-co-CrA, and **h** St-co-CrA/Na

earlier degradation, likely due to decarboxylation effects. Metal complexation, particularly with Fe(III) and Cu(II), improves thermal stability by forming stable metal–oxygen bonds, increasing decomposition temperatures to 425–450 °C due to cross-linking. The enhanced crystallinity and higher glass transition temperatures, particularly in the St-co-CA complexes, are linked to the rigidity and structural order induced by the cinnamic acid moieties. This study highlights the critical role of metal coordination in boosting thermal properties, making these materials promising candidates for applications requiring high thermal resistance.

The copolymers demonstrated a strong affinity for complex formation with copper, cobalt, and iron and exhibited semiconducting behavior with conductivity values ranging from 10^{-3} to 10^{-6} Ω^{-1} cm^{-1} when their electrical properties were measured. In short, the presented research study emphasizes the importance of the electrical properties of chelating copolymers and their metal complexes, with particular emphasis on binary chelating copolymers of styrene, in modern technologies and the advancement of science and the economy.

6 Future research directions and potential applications

Future research could explore the coordination of other metal ions (e.g., nickel, zinc) to enhance the electrical conductivity and thermal stability of the copolymers. Additionally, optimizing the ratio of maleic, cinnamic, and crotonic acids may improve their mechanical properties for broader industrial use. Potential applications include organic electronics, sensors, and energy storage devices like batteries. These copolymers may also serve as eco-friendly materials for green coatings, conductive inks, and corrosion resistance. Further studies on their electrochemical stability and long-term performance could boost their industrial scalability and impact.

Abbreviations

Characterization techniques

FTIR	Fourier transform infrared
^{1}H-NMR	Proton nuclear magnetic resonance powder
PXRD	X-ray diffraction
TGA	Thermogravimetric analysis
DSC	Differential scanning calorimetry

Binary copolymers

St-Co-MA	Styrene with maleic acid
St-Co-CA	Styrene with cinnamic acid
St-Co-CrA	Styrene with crotonic acid

Supplementary Information

The online version contains supplementary material available at https://doi.org/10.1186/s43088-024-00583-w.

Additional file 1

Acknowledgements
The authors acknowledge the scientific contribution and supporting by their research institutions.

Author contributions
Mohamed Yahia (M.Y.), Dalia Refaat (D.R), Gaber El-Enany (G.M.E.-E), and Mahmoud Abd El-Ghaffar (M.A.E.-G): Conceptualization, methodology, software, validation, formal analysis, investigation, resources, data curation, writing—original and final draft, review and editing, visualization, supervision, and funding acquisition.

Funding
No external funding was obtained for this research.

Availability of data and materials
Data are enclosed within the article and supplementary materials.

Declarations

Ethics approval and consent to participate
No applicable.

Consent for publication
Not applicable.

Competing interests
The authors of this work have stated that there is no conflict of interest to declare.

Author details
[1]Chemistry Department, Faculty of Science, Helwan University, Cairo 11795, Egypt. [2]Center for Cooperative Research On Alternative Energies (CIC energiGUNE), Basque Research and Technology Alliance (BRTA), Alava Technology Park, Albert Einstein 48, 01510 Vitoria-Gasteiz, Spain. [3]Instituto de Nanociencia y Materiales de Aragón (INMA), CSIC-Universidad de Zaragoza, 50018 Zaragoza, Spain. [4]Chemical and Environmental Engineering Department, Universidad de Zaragoza, 50018 Zaragoza, Spain. [5]Scientific Department, Engineering Faculty, Port Said University, Port Said 42526, Egypt. [6]Physics Department, Science and Arts College of Uqlat Alsuqor, Qassim University, Buraydah, Saudi Arabia. [7]Department of Polymer and Pigment, National Research Center, Dokki, Cairo 12622, Egypt.

Received: 8 January 2024 Accepted: 23 November 2024
Published online: 10 December 2024

References

1. Kaliyappan T, Kannan P (2000) Co-ordination polymers. Prog Polym Sci 25:343–370
2. Zhang W, Aguila B, Ma S (2017) Retracted article: potential applications of functional porous organic polymer materials. J Mater Chem A 5:8795–8824
3. Rivas BL, Seguel GV, Ancatripai C (2000) Polymer-metal complexes: synthesis, characterization, and properties of poly(maleic acid) metal complexes with Cu(II), Co(II), Ni(II), and Zn(II). Polym Bull 44:445–452

4. Mortimer RJ (2011) Electrochromic materials. Annu Rev Mater Res 41:241–268
5. Hegazy E-SA, Dessouki AM, El-Assy NB, El-Sawy NM, El-Ghaffar MA (1992) A. Radiation-induced graft polymerization of acrylic acid onto fluorinated polymers. I. Kinetic study on the grafting onto poly(tetrafluoroethylene-ethylene) copolymer. J Polym Sci Part A Polym Chem 30:1969–1976
6. Saha B, Iglesias M, Dimming I, Streat M (2000) Sorption of trace heavy metals by thiol containing chelating resins. Solvent Extr Ion Exch 18:133–167
7. Menoud P, Cavin L, Renken A (1998) Modelling of heavy metals adsorption to a chelating resin in a fluidized bed reactor1Dedicated to Professor K.R. Westerterp on occasion of his 70th birthday.1. Chem. Eng. Process. Process Intensif. 37:89–101
8. Alexandratos SD, Smith SD (2004) High stability solvent impregnated resins: metal ion complexation as a function of time. Solvent Extr Ion Exch 22:713–720
9. Amphlett JTM, Choi S, Parry SA, Moon EM, Sharrad CA, Ogden MD (2020) Insights on uranium uptake mechanisms by ion exchange resins with chelating functionalities: chelation vs. anion exchange. Chem. Eng. J. 392:123712
10. Dzhardimalieva GI, Uflyand IE (2017) Review: recent advances in the chemistry of metal chelate monomers. J Coord Chem 70:1468–1527
11. El-Sawy NM, Al Sagheer F (2001) Radiation-induced graft polymerization of acrylic acid onto poly(tetrafluoroethylene-perfluorovinyl ether) copolymer films: complexation with some transition metals and biological activity. Eur Polym J 37:161–166
12. Tsurugi H, Mashima K (2019) Salt-free reduction of transition metal complexes by Bis(trimethylsilyl)cyclohexadiene, -dihydropyrazine, and -4,4′-bipyridinylidene derivatives. Acc Chem Res 52:769–779
13. Nanjundan S, Selvamalar CSJ, Jayakumar R (2004) Synthesis and characterization of poly(3-acetyl-4-hydroxyphenyl acrylate) and its Cu(II) and Ni(II) complexes. Eur Polym J 40:2313–2321
14. Jakubiak A, Owsik IA, Kolarz BN (2005) The oxidation of hydroquinone catalysed by Cu(II) ions immobilized on acrylic resins. The influence of ionic liquid. React Funct Polym 65:161–167
15. Kolarz BN, Jakubiak A, Jezierska J, Dach B (2008) Polymeric supports with amino groups from halogenoacetylated styrene/divinylbenzene copolymers. React Funct Polym 68:1207–1217
16. Gupta KC, Sutar AK (2008) Catalytic activities of polymer-supported metal complexes in oxidation of phenol and epoxidation of cyclohexene. Polym Adv Technol 19:186–200
17. Gupta K, Sutar AK (2008) Catalytic activity of polymer anchored N, N′-bis (o-hydroxy acetophenone) ethylene diamine Schiff base complexes of Fe (III), Cu (II) and Zn (II) ions in oxidation of phenol. Reactive Funct Polym 68:12–26
18. Guibal E, Vincent T, Touraud E, Colombo S, Ferguson A (2006) Oxidation of hydroquinone to p-benzoquinone catalyzed by Cu (II) supported on chitosan flakes. J Appl Polym Sci 100:3034–3043
19. Kaliyappan T, Kannan P (1996) Synthesis, spectral and thermal properties of poly (2-hydroxy-4-methacryloyloxybenzaldehyde)-metal complexes. J Polym Sci Part A Polym Chem 34:3551–3557
20. Zeng X, Zhang Y, Shen Z (1997) Ring opening polymerization of propylene oxide by chitosan-supported rare earth catalytic system and its kinetics. J Polym Sci Part A Polym Chem 35:2177–2182
21. Dragan ES, Dinu MV, Lisa G, Trochimczuk AW (2009) Study on metal complexes of chelating resins bearing iminodiacetate groups. Eur Polym J 45:2119–2130
22. Dörr JM, Scheidelaar S, Koorengevel MC, Dominguez JJ, Schäfer M, van Walree CA, Killian JA (2016) The styrene–maleic acid copolymer: a versatile tool in membrane research. Eur Biophys J 45:3–21
23. Kopf AH, Koorengevel MC, van Walree CA, Dafforn TR, Killian JA (2019) A simple and convenient method for the hydrolysis of styrene-maleic anhydride copolymers to styrene-maleic acid copolymers. Chem Phys Lipids 218:85–90
24. Smith AA, Autzen HE, Laursen T, Wu V, Yen M, Hall A, Hansen SD, Cheng Y, Xu T (2017) Controlling styrene maleic acid lipid particles through RAFT. Biomacromol 18:3706–3713
25. Solomko NY, Dron I, Budishevskaya O, Voronov S (2009) Emulsion polymerization of vinyl monomers in presence of chitosan with peroxide groups. Procedia Chem 1:1567–1575
26. Kostjuk SV, Ganachaud F (2010) Cationic polymerization of vinyl monomers in aqueous media: From monofunctional oligomers to long-lived polymer chains. Acc Chem Res 43:357–367
27. Yamamoto T (2012) Soap-free emulsion polymerization of aromatic vinyl monomer using AIBN. Colloid Polym Sci 290:1833–1835
28. Morlay C, Mouginot Y, Cromer M, Vittori O (2002) The removal of Cu (II), Cd (II), Ni (II) and Pb (II) from dilute aqueous solution by a poly (acrylic acid) flocculant and its cross-linked analogue. Water Sci Technol Water Supply 2:27–34
29. Morlay C, Cromer M, Mouginot Y, Vittori O (1998) Potentiometric study of Cu (II) and Ni (II) complexation with two high molecular weight poly (acrylic acids). Talanta 45:1177–1188
30. Yokoi H, Kawata S, Iwaizumi M (1986) Interaction modes between heavy metal ions and water-soluble polymers. 2. Spectroscopic and magnetic reexamination of the aqueous solutions of cupric ions and poly (acrylic acid). J Am Chem Soc 108:3361–3365
31. Abd El-Ghaffar M, Badran A, Shendy S (1992) Preparation and evaluation of some homo and copolymeric emulsions for latex paint applications. J Elastomers Plast 24:192–202
32. El-Ghaffar MAA, Youssef EAM, El-Halawany NR (2002) Preparation and characterization of some acrylic acid chelating copolymers by emulsion techniquE. J Macromol Sci Part A 39:1037–1059
33. Patel M, Patil S (1983) The preparation and characterization of some polyschiff base complexes. Synth React Inorg Met-Org Chem 13:133–144
34. El-Shekeil A, Khalid MA, Al-Maydama H, Al-Karbooly A (2001) DC electrical conductivity of polydithiooxamide–metal complexes. Eur Polym J 37:575–579
35. Dutta P, Biswas S, Ghosh M, De S, Chatterjee S (2001) The dc and ac conductivity of polyaniline–polyvinyl alcohol blends. Synth Met 122:455–461
36. Mott NF, Davis EA (2012) Electronic processes in non-crystalline materials. Oxford University Press, Oxford, UK
37. Luo J, Cheng D, Li M, Xin M, Sun W, Xiao W (2020) RAFT copolymerization of styrene and maleic anhydride with addition of ascorbic acid at ambient temperature. Adv. Polym. Technol. 2020:3695234
38. Bag S, Ghosh S, Paul S, Khan ME, De P (2021) Styrene-maleimide/maleic anhydride alternating copolymers: recent advances and future perspectives. Macromol. Rapid Commun. 42:2100501
39. Singh N, Riaz U (2022) Recent trends on synthetic approaches and application studies of conducting polymers and copolymers: a review. Polym Bull 79:10377–10408
40. McCullough LA, Matyjaszewski K (2010) Conjugated conducting polymers as components in block copolymer systems. Mol Cryst Liq Cryst 521(1):1–55

Publisher's Note